DISLOCATION MODEL FOR FATIGUE CRACK PROPAGATION OF LONG CRACKS

REINHARD PIPPAN, FRANZ O. RIEMELMOSER

The differences between the description of cyclic plasticity with a discrete dislocation model and the classical elasto-plastic continuum theory are studied. It is shown that both the dislocation model and the continuum mechanics lead to the same results at high stress intensity ranges (Paris regime) but they differ significantly for small stress intensity ranges. The conclusion of these results is that the characteristics of the near-threshold fatigue-crack-growth behavior is only explainable with a discrete dislocation model.

1. Introduction

It is widely accepted that the central mechanism leading to fatigue crack propagation is the cyclic plastic deformation at the crack tip. For large stress intensity factors, i.e. in the mean and upper Paris regime, the plastic deformations are large and the crack tip plasticity can be described by classical elasto-plastic continuum theories. At small stress intensity ranges, in the near threshold regime, the situation is different. Here the plastic zone is confined to a very small region in front of the crack and the cyclic plastic deformations are only of the order of a few Burgers vectors. We will show that here the classical elasto-plastic continuum mechanics is not appropriate to describe the plasticity at the crack tip. In the near threshold regime the plasticity is strongly influenced by its discrete (dislocation) nature.

Detailed investigations of the interaction of single dislocations with a crack tip have been performed already in the mid-eighties where the attention was at first focused to the ductile-to-brittle transition of metals [1–16]. In the early nineties the dislocation-crack investigations have been extended to cyclically loaded cracks [17–30].

In the first step the threshold conditions of the cyclic plastic deformation in front of a mode II and a mode III crack were studied in dependence on the chosen stress intensity factor necessary to generate a dislocation and on the friction stress. Also, the influence of dislocation obstacles was taken into consideration [24, 25]. A stationary (non propagating) mode I crack was investigated in [26, 28, 30]. There we compared the results of the discrete dislocation model with the predictions of

Doz. Dr. R. Pippan, Dr. F. O. Riemelmoser, Erich Schmid Institute, Austrian Academy of Sciences, Jahnstr. 12, A-8700 Leoben, Austria.

a continuum mechanics analysis. In [28, 30] the dislocation model was extended to describe a growing fatigue crack where dislocations accumulate in the wake.

The purpose of the present paper is to summarize the fundamental assumptions in such dislocation based models and to give an overview of the most important results.

2. Fundamentals

In our simulations the crack tip plasticity is described by generation and motion of geometrically necessary dislocations [28]. A schematic dislocation arrangement for the three loading modes is depicted in Fig. 1. A mode I loading causes the motion of edge dislocations in symmetric and inclined slip planes. At mode II and mode III cracks edge respectively screw dislocations are arranged directly ahead of the crack tip.

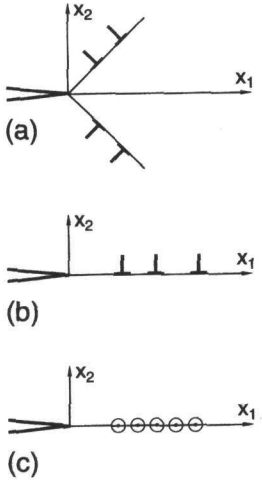

Fig. 1. Dislocation arrangement at a mode I (a) mode II (b) and mode III (c) crack.

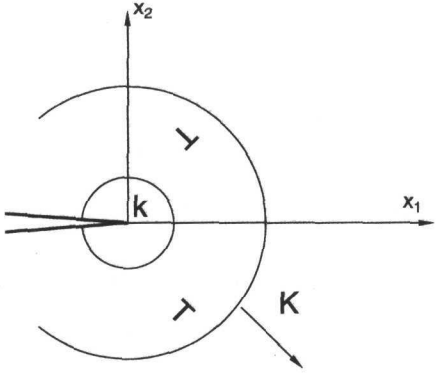

Fig. 2. Schematic illustration of the zones which are dominated by the local stress intensity factor k and the applied or global stress intensity factor K if dislocations are present in front of the crack.

a) *The local and the global stress field*

At a linear elastic crack there exists a zone at the crack tip where the stress intensity factor is a unique measure of the stress field. If now the crack is loaded

and dislocations enter this region the stresses are changed. It can be shown [8] that this new stress field is characterized now by two stress intensity factors, as sketched in Fig. 2. At distances much larger than the plastic zone size the stresses are given by a global stress intensity factor, K. Very near the crack tip, at distances smaller than the distance between crack tip and the closest dislocation, the stress field is determined by a local stress intensity factor, k. The relation between both stress intensity factors is given by

$$k = K + \sum k_d,$$

where k_d is the stress intensity factor induced by a single dislocation [8]. The summation in the equation above is performed over all dislocations in the plastic zone. Note that we use capital letters to designate global or applied parameters, to label local ones we use small letters. The difference between K and k, i.e. the sum over k_d, is called shielding stress intensity k_s of the dislocations [3, 29].

The stresses in the transient region between the two stress intensity dominated fields are determined by the dislocation arrangement and the applied stress intensity factor. The size of the transient zone is of the order of the plastic zone size. A crack is called long if this transient region is small in comparison to the crack length. In this case the stress intensity factor K, the stress intensity range ΔK, the stress ratio R, the friction stress (or yield stress), and the dislocation generation mechanism determine what happens during monotonic and cyclic loading.

b) *Dislocation source*

We confine our considerations to small stress intensity factors. As a consequence, the plasticity is bounded to the immediate vicinity of the crack tip. In this small region internal dislocation sources (e.g., Frank-Read sources) are not available. We assume that the dislocations are generated at the crack tip. This source mechanism was discussed by Rice and Thomson [8] and further elaborated by Schöck [12] and Rice [32]. Their analyses show that spontaneous dislocation emission at the crack tip occurs when the local stress intensity factor reaches a critical value k_e. In [27] a different dislocation generation mechanism was assumed. There the dislocations are generated somewhat ahead of the crack tip at a conventional dislocation source. A comparison of the results in [27] with our simulations shows that the principal conclusions are the same in both models. In the case of internal dislocation sources only additional parameters like the position and the critical stress of the dislocation mills have to be taken into account.

c) *Dislocation reaction and moving conditions*

A single dislocation in an unbounded linear elastic medium does not feel the force from itself. If additional stress sources are applied a Peach-Kochler force acts

on the dislocation

$$\mathrm{d}\boldsymbol{f} = (\sigma \cdot \boldsymbol{b}) \times \mathrm{d}\boldsymbol{l},$$

where $\boldsymbol{b}$ is the Burgers vector, σ is the stress tensor and $\mathrm{d}\boldsymbol{f}$ is the force on the line segment $\mathrm{d}\boldsymbol{l}$. In our simulations the additional stress sources are the following:

– the stresses caused by the applied stress intensity factor,

– the stresses caused by the free surface (the crack), which is called the image stress,

– the stresses caused by the other dislocations.

In the model the dislocations are not allowed to change their glide plane such that their motion is controlled by the slip force. A dislocation is at rest whenever the slip force is less than the friction stress (or a certain critical stress if it is located at an obstacle) otherwise the dislocation moves into the direction of the slip force. Two dislocations with opposite Burgers vectors annihilate when their mutual distance shrinks to a certain limit. Dislocations returning to the crack disappear at the free surface.

3. A typical load cycle

In order to demonstrate what happens during a fatigue cycle, the change of the local and the applied stress intensity, as well as the crack-tip opening displacement are shown in Fig. 3a,b for mode III. In this example we assume a critical stress intensity for emission of a screw dislocation being $k_e = 0.15\mu\sqrt{b}$ and a friction stress $\sigma_F = 0.001\mu$ which are typical for metals. Since the assumed moving conditions for dislocations are independent of the loading rate, we can use arbitrary units for the time scale.

In our computer simulation the applied stress intensity is increased (and decreased in the case of unloading) in steps. After each step, the conditions for dislocation emission are controlled and the equilibrium position for every dislocation is calculated. At the beginning of the loading there are no dislocations in front of the crack. Hence, for K values smaller than k_e the local and applied stress intensity are equal. As soon as the applied stress intensity factor reaches the critical stress intensity k_e, the first dislocation is emitted and glides away from the crack tip. It reaches its equilibrium position where the shear stress acting at the position of the dislocation is smaller than the friction stress. The emission of the dislocation causes an "opening" (shearing) of the crack tip of 1 Burgers vector. This is one of the essential differences between the discrete dislocation model and the classical continuum mechanics. In the dislocation model there is a minimum load necessary to produce plastic flow whereas continuum mechanics predicts even at such small stress intensity ranges a non vanishing plastic deformation.

The generated dislocation in front of the tip reduces the local stress intensity factor. The further increase of the applied stress intensity factor causes a motion of

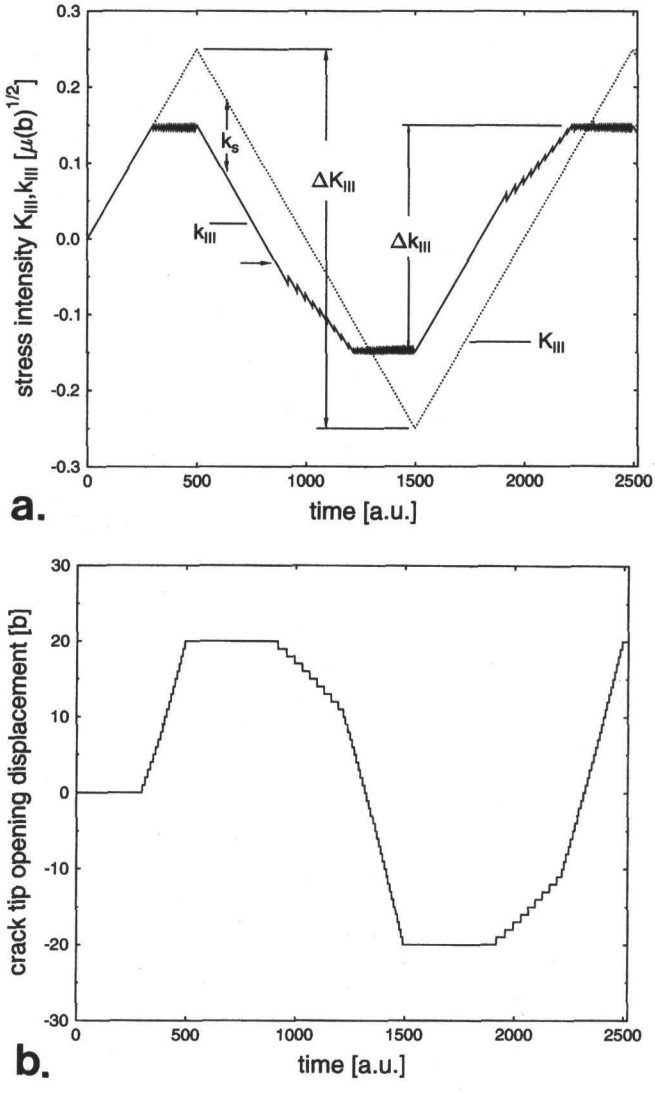

Fig. 3. Change of the applied and local stress intensity of a mode III crack during cyclic loading at the stress ratio $R = -1$, for $k_e = 0.15\mu\sqrt{b}$ and $\sigma_F = 0.001\mu$ (a) and the change of the corresponding crack tip opening displacement (b).

the first dislocation away from the crack tip. The local stress intensity increases to k_e and the second dislocation is emitted. This leads to a further plastic "opening" at the crack tip.

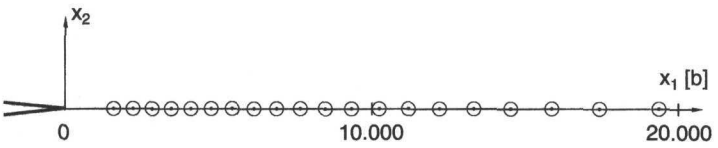

Fig. 4. Dislocation distribution in the slip plane ahead of a mode III crack at $K_{\max} = 0.25\mu\sqrt{b}$, $\sigma_F = 0.001\mu$, $k_e = 0.15\mu\sqrt{b}$.

These processes continue till one reaches $K_{\max}$. The arrangement of the dislocations at $K_{\max}$ is depicted in Fig. 4. It looks like an inverse pile-up of dislocations, with a dislocation free zone near the crack tip. This is a characteristic result of the assumed dislocation source (but also for Frank-Read sources the arrangement is very similar [28]). The dislocation free zone is the second significant difference between dislocation model and the continuum mechanics. The latter predicts a 1/radius singularity in the plastic strains at the crack tip.

Let us now consider what happens during unloading. At $K_{\max}$ the stress acting on each dislocation (in Fig. 4) is equal to the friction stress. During unloading these stresses are reduced. However, the dislocation can move towards the crack tip only when the shear stress at their positions is smaller than the negative friction stress. For that reason the dislocation arrangement is not changed in the very first unloading phase. Here the system behaves purely elastically. This means the crack tip opening displacement is not changed. After a certain unloading the stress acting on the last emitted dislocation becomes smaller than the negative friction stress and this dislocation moves towards the crack tip. As a consequence the local stress intensity factor decreases faster than the global one. The effect however is so small that it cannot be seen in Fig. 3a. Therefore, the stress intensity factor where the closest dislocation starts moving towards the crack tip is marked by an arrow. When the closest dislocation reaches a certain distance to the crack tip, it returns spontaneously to the free surface and disappears. The plastic crack tip opening displacement is reduced by one Burgers vector. Caused by the return of the dislocation, the total dislocation shielding decreases and the local stress intensity factor increases. During further unloading more and more dislocations move back to the crack until the criterion to emit a dislocation with an opposite sign of the Burgers vector is satisfied. This happens when the local stress intensity factor decreases to $k = -k_e$.

The first emitted "negative" (unloading) dislocation recombines with the "positive" (loading) dislocation. The emission of a negative dislocation and the annihilation of a pair of dislocations is seen in the local k vs. time curve as a small step. The generation of negative dislocations and the annihilation of dislocation

pairs continues until the positive dislocations are exhausted. From now on, the dislocation arrangement and the change of the local stress intensity is the same as in the loading sequence where only the loading direction and the sign of the Burgers vector is changed. Since the maximum stress intensity in the unloading sequence is assumed to be $-K_{\max}$ the dislocation arrangement at the negative maximum load is identical to that of the positive maximum load. (This is true for the simulations of mode II and mode III cracks. In case of a mode I crack the symmetry between loading and unloading cycle is lost due to the crack-flank contact during unloading.) In the following loading phase, the same processes as just described are repeated with a changed sign of the Burgers vector.

4. The cyclic crack tip opening displacement as a function of the stress intensity range

Fig. 5 shows the ΔCTOD as a function of the far field stress intensity range (solid curve) for a stationary mode I crack. The crack is not allowed to propagate during the cyclic loading, and there are no dislocations in its wake. The following parameters are assumed for this calculation [26]: symmetric dislocation arrangement as depicted Fig. 1a, angle of dislocation emission $\alpha = 70.53°$, shear modulus $\mu = 80{,}000$ MPa, $k_e = 0.4\mu \cdot \sqrt{b}$, $\sigma_F = \mu/200$, $R = 0$.

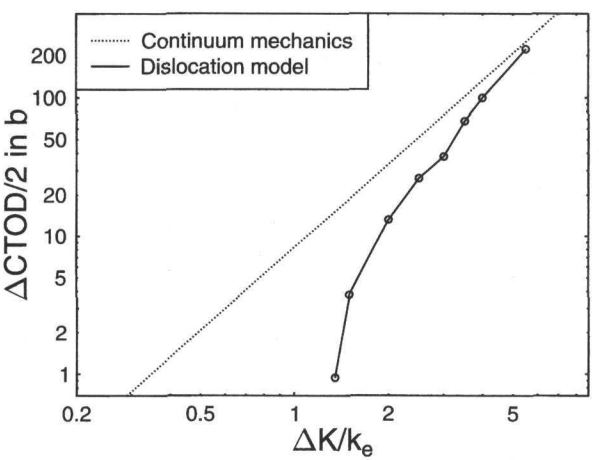

Fig. 5. Cyclic crack tip opening displacement, ΔCTOD, in units of Burgers vectors as a function of $\Delta K/k_e, R = 0$, for mode I loading.

The dotted line in Fig. 5 is the continuum mechanics prediction of the ΔCTOD based on Rice's slip line model [31]. A comparison between both curves shows

that for large ΔK values both Rice's slip line model and the discrete dislocation model lead to the same result. For small ΔK values large differences appear. The differences are primarily due to the absence of plasticity in the discrete dislocation model at the very beginning of the loading and the unloading cycle. In continuum mechanics even the smallest change in the loading conditions leads to a plastic flow.

Let us assume that ΔCTOD is proportional to $\mathrm{d}a/\mathrm{d}N$. In this case Fig. 5 can be interpreted as an intrinsic crack growth curve (note that it is plotted in a $\log \Delta$CTOD vs. $\log \Delta K$ diagram). The continuum mechanics predicts a linear relation between log "crack growth rate" and $\log \Delta K$ whereas the discrete dislocation model shows the real observed threshold behaviour.

Fig. 6 shows again a calculated ΔCTOD vs. ΔK diagram based on the discrete dislocation model for a mode III crack as depicted in Fig. 1c. The parameters assumed in the computer simulation are $R = 0.1$, $k_e = 0.2\mu\sqrt{b}$ and the friction stress 0.0005μ (open circles) and 0.002μ (full circles). The comparison of the mode I and the mode III simulations leads to the following conclusions:

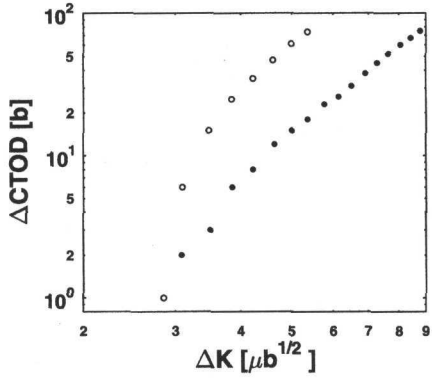

Fig. 6. Influence of the friction stress on the cyclic crack tip opening displacement in units of Burgers vectors as a function of ΔK, $R = 0.1$, mode III crack, $k_e = 0.2\mu\sqrt{b}$, $\sigma_F = 0.0005\mu$ (black circles) and 0.002μ (white circles).

– The loading mode does not influence the general behaviour of the ΔCTOD versus ΔK curve.

– In the Paris regime the ΔCTOD values are proportional to $1/\sigma_F$ which is in agreement with the prediction of the elasto-plastic continuum mechanics.

– In the near threshold regime the influence of the friction stress on the ΔCTOD vs. ΔK curve vanishes. The dislocation generation mechanism is the dominant process in this case. This means that the onset of the cyclic plasticity, and hence, the intrinsic threshold for fatigue crack propagation is determined by the dislocation generation mechanism.

5. The propagating crack

In principle, different propagation mechanisms can be assumed in the computer simulation for fatigue crack propagation. In our simulation [28] of a mode I crack, we use a blunting model which is similar to Pelloux' crack growth model [33] and to the stereophotogrammetric observations of Bichler [34]. In the loading sequence the crack emits dislocations whereby the crack blunts and grows. The crack growth

increment per emission of one dislocation is $\Delta a = |b| \cdot \cos\alpha$, where α is the angle between the growing direction and the slip plane.

Fig. 7 shows the calculated dislocation arrangement of a propagating crack. The material parameters are the same as those used for the simulation of the stationary fatigue crack. The details of the calculations and results are given in [30]. The most important difference between the continuum mechanics description and the discrete dislocation modelling is the inhomogeneity of the deformation which can be seen clearly in Fig. 7. Under steady state conditions the dislocation in the wake of a propagating crack arrange in slip bands which are separated by dislocation free regions. The distance between the slip bands cannot become arbitrarily small. The reason is the long range elastic interaction force between the dislocations. A very important consequence of this effect is that each slip band leaves a slip step on the fracture surface which to our belief is the reason for the so called abnormal striation spacing in the near threshold regime.

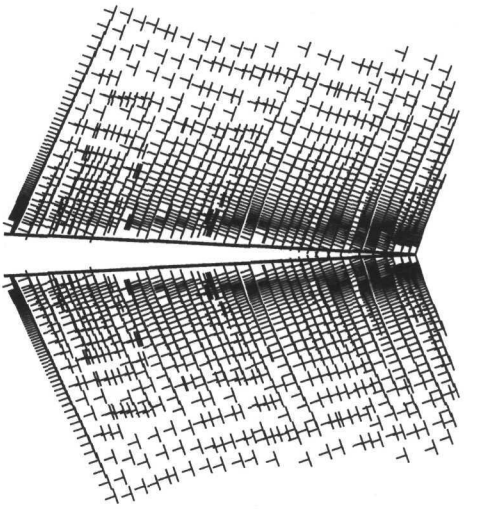

Fig. 7. Arrangement of edge dislocations in the wake of a growing mode I (tearing) crack, $K_{max} = 4k_e$, the parameters for the calculation are the same as in Fig. 5.

6. Conclusion

In this paper the principles of modelling the dislocation motion during fatigue crack propagation are discussed. We consider mode I, mode II, and mode III cracks. In the last case the generated dislocations are screw dislocations, in the former cases edge dislocations are produced during the cyclic loading. The comparison of these simulations revealed that the CTOD-ΔK curves are similar in the three loading modes. In particular, the ΔCTOD at large stress intensity ranges is proportional to the lattice friction stress and at small stress intensity ranges the ΔCTOD-ΔK curves bend down leading to a threshold of the plastic deformation at a ΔCTOD of 1 Burgers vector per cycle. This explains the intrinsic threshold behaviour of fatigue cracks and it shows the necessity to model here the plastic deformation as motion of discrete dislocations.

Acknowledgements. This work was supported by the Fonds zur Förderung der wissenschaftlichen Forschung P11622 TEC.

REFERENCES

[1] OHR, S. M.—NARAYAN, J.: Philosophical Magazine, *A 41*, 1980, p. 81.
[2] KOBAYASHI, S.—OHR, S. M.: Journal of Materials Science, *19*, 1984, p. 2273.
[3] OHR, S. M.: Materials Science Engineering, *72*, 1985, p. 1.
[4] NARITA, N.—HIGASHIDA, K.—KITANO, S.: Scripta Metallurgica, *21*, 1987, p. 1273.
[5] CHIA, K. Y.—BURNS, S.: Scripta Metallurgica, *18*, 1984, p. 467.
[6] FOECKE, T.—GERBERICH, W. W.: Scripta Metallurgica, *24*, 1990, p. 535.
[7] NARITA, N.—HIGASHIDA, K.—TORII, T.—MIYAKI, S.: Materials Transactions, JIM 30, 1989, p. 895.
[8] RICE, J. R.—THOMSON, R.: Philosophical Magazine, *29*, 1974, p. 73.
[9] WEERTMAN, J.: Philosophical Magazine, *43*, 1981, p. 1103.
[10] CHIAO, Y. H.—CLARKE, D. R.: Acta Metallurgica, *37*, 1989, p. 203.
[11] LIN, I. H.—THOMSON, R.: Acta Metallurgica, *34*, 1986, p. 187.
[12] SCHÖCK, G.: Philosophical Magazine, *A 63*, 1991, p. 111.
[13] HIRSCH, P. B.—ROBERTS, S. G.—SAMUELS, J.: Scripta Metallurgica, *21*, 1987, p. 1523.
[14] MAJUMDAR, B. S.—BURNS, S. J.: Acta Metallurgica, *29*, 1981, p. 579.
[15] SHIUE, S. T.—LEE, S.: Journal of Physics D: Applied Physics, *22*, 1989, p. 1708.
[16] LI, W. L.—LI, J. C. M.: Philosophical Magazine, *A 59*, 1989, p. 1245.
[17] HORTON, J. A.—OHR, S. M.: Scripta Metallurgica, *16*, 1982, p. 621.
[18] WEERTMAN, J.: In: Mechanics of Fatigue. Ed.: Mura, T. New York, ASME 1981, p. 11.
[19] LI, J. C. M.: Scripta Metallurgica, *20*, 1986, p. 1477.
[20] PIPPAN, R.: Scripta Metallurgica, *23*, 1989, p. 1575.
[21] LI, J. C. M.: In: Dislocations of Solids: Some Recent Advances. Ed.: Markenscoff. American Society of Mechanical Engineers, *63*, 1984, p. 35.
[22] MURA, T.—WEERTMAN, J.: In: Proceedings Fatigue Crack Growth Threshold Concepts. Eds.: Davidson and Suresh. Warrendale, AIME, PA 1984, p. 531.
[23] LI, J.—LI, J. C. M.: Materials Science Engineering, *A 129*, 1990, p. 167.
[24] PIPPAN, R.: Acta Metallurgica Materialia, *39*, 1991, p. 255.
[25] PIPPAN, R.: International Journal of Fracture, *58*, 1992, p. 305.
[26] RIEMELMOSER, F. O.—PIPPAN, R.—STÜWE, H. P.: International Journal of Fracture, *85*, 1997, p. 157.
[27] WILKINSON, A. J.—ROBERTS, S. G.—HIRSCH, P. B.: Acta Materialia, *46*, 1998, p. 379.
[28] RIEMELMOSER, F. O.—PIPPAN, R.—STÜWE, H. P.: Acta Materialia, 1998, in print.
[29] PIPPAN, R.—RIEMELMOSER, F. O.: Zeitschrift für Metallkunde, *86*, 1995, p. 823.
[30] RIEMELMOSER, F. O.—PIPPAN, R.: Materials Science and Engineering A, 1997, p. A234.
[31] RICE, J. R.: American Society of Testing Materials, ASTM STP 415, 1967, p. 247.
[32] RICE, J. R.: Mechanics and Physics of Solids, *40*, 1992, p. 239.
[33] PELLOUX: Trans. Am. Soc. Met., *62*, 1962, p. 76.
[34] BICHLER, CH.: Rißspitzenverformung bei konstanter und variabler Amplitude. [Thesis]. Leoben, 1997.